actuators

MDPI

Article

A Practical Deceleration Control Method, Prototype Implementation and Test Verification for Rail Vehicles

Tianhe Ma [1,2], Chun Tian [2,*], Mengling Wu [2], Jiajun Zhou [2] and Yinhu Liu [3]

[1] Postdoctoral Station of Mechanical Engineering, Tongji University, Shanghai 201804, China; math@tongji.edu.cn
[2] Institute of Rail Transit, Tongji University, Shanghai 201804, China
[3] CRRC Nanjing Puzhen Haitai Brake Equipment Co., Ltd., Nanjing 211800, China
* Correspondence: chtian@tongji.edu.cn

Abstract: Currently, the theoretical braking force control mode, characterized by actual deceleration as an unstable open-loop output, is the most widely used brake control mode in trains. To overcome the shortcomings of non-deceleration control modes, a deceleration control mode is proposed to realize the closed-loop control of train deceleration. First, a deceleration control algorithm based on parameter estimation was derived. Then, the deceleration control software logic was designed based on the existing braking system to meet the engineering requirements. Finally, the deceleration control algorithm was verified through a ground combination test bench with real brake control equipment and pneumatic brakes. The test results show that the deceleration control can make the actual braking deceleration of the train accurately track the target deceleration in the presence of disturbances, such as uncertain brake pad friction coefficients, line ramps, vehicle loads and braking force feedback errors, as well as their combined effects, and does not affect the original performance of the braking system. The average deceleration in the deceleration control mode is relatively stable, and the control error of instantaneous deceleration is smaller.

Keywords: train braking; braking control; deceleration control; parameter estimation; hardware-in-the-loop test

Citation: Ma, T.; Tian, C.; Wu, M.; Zhou, J.; Liu, Y. A Practical Deceleration Control Method, Prototype Implementation and Test Verification for Rail Vehicles. *Actuators* **2023**, *12*, 128. https://doi.org/10.3390/act12030128

Academic Editor: Hai Wang

Received: 12 February 2023
Revised: 13 March 2023
Accepted: 15 March 2023
Published: 17 March 2023

1. Introduction

Urban rail transit plays a vital role in the modern transportation systems of many big cities. Braking deceleration is one of the most important performance indices for metro trains. When the train is braking, the braking force is calculated according to the braking command and then applied by the braking systems. If there are no uncertain parameters or other disturbances, the braking deceleration is consistent with the target deceleration decided by the command signal. However, because the train in operation is always affected by factors, such as uncertain ramps, friction coefficients, running resistance, load variations and sensor errors, the actual deceleration often deviates from the target value [1]. The precision of the deceleration is the foundation of proper braking distance and stopping accuracy [2]. Excessive deceleration may reduce the comfort of passengers, while too-small a deceleration may affect the safe distance of train operation [3]. Hence, currently, the closed-loop deceleration control rather than the conventional theoretical braking force control is becoming increasingly attractive [4,5].

Research has been carried out to improve the stability and accuracy of the vehicle braking process. Nankyo et al. [6–8] proposed a PI controller with a Smith predictor for deceleration feedback control. The time delay and first-order lag of pneumatic braking systems were considered. Based on the train information management system (TIMS), the closed-loop control of the actual braking deceleration of the train was realized by adjusting the braking force of the entire train. However, this type of method has no perception of the interference factors that cause deceleration deviation. Additionally, it is difficult to

set the parameters of the Smith predictor appropriately. Furthermore, Nakazawa et al. [9] proposed a new method that produces online deceleration updates based on the current braking distance and the target distance, compensating for deceleration decline when an effective braking force is lost in low-adhesion conditions and preventing the extension of braking distance.

Wu et al. [4] determined a trend in deceleration control for railway vehicles, proposing that the actual braking deceleration of the train can be approximately replaced with the absolute longitudinal deceleration. In follow-up studies, the team designed deceleration control methods based on the recursive least-square estimator with speed feedback [10–12], which is an improved Smith predictor method [13] and a gradient estimator [14] with deceleration feedback. On this basis, this paper simplifies the above-mentioned methods to render them easy for engineering realization, develops a brake controller prototype and conducts the 1:1 ground combination test.

There are other studies about deceleration control and train operation control. Zhang et al. [15] proposed a deceleration controller based on the Lyapunov–Krasovskii method and backstepping technique. Yin et al. [16] developed two train operation control algorithms with one based on expert rules and the heuristic expert inference method and the other based on reinforcement learning. These methods can improve operation punctuality and reduce energy consumption. Wang et al. [17,18] proposed a model predictive controller (MPC) and improved the softness-factor-obtaining method with a whale optimization algorithm. Additionally, a predictive function control algorithm with step function and Morlet function as the basis functions was also studied. Tan et al. [19] adopted the model reference adaptive control strategy to realize the tracking of the given speed curve, which can overcome the problems of unknown disturbance and input time lag. Li et al. [20] established a distributed three-order autoregressive model for the braking process of EMU trains and designed a multivariable generalized predictive control method to achieve speed tracking control by generating the braking force of each car. These studies can be described as tracking problems of train velocity or deceleration profiles. Tracking the deceleration curve or, in other words, the precise control of actual deceleration is the basis of train braking operation.

The target value of train braking force is generated by the upper controller and is applied by actuators, such as pneumatic or hydraulic calipers. Therefore, a hierarchical control architecture is necessary. Nie et al. [21] proposed a hierarchical controller for an electric vehicle to actively control the braking deceleration. Luo et al. [22–24] built a detailed electro-pneumatic brake model and developed a sliding-mode pressure controller. Pneumatic braking systems are also utilized in heavy-duty road vehicles, and the stopping precision of these vehicles is also a key issue. Bu et al. [25] adopted an indirect adaptive control technology to decouple feedback control and parameter estimation, thus improving the parking accuracy of heavy-duty vehicles. Additionally, some renowned braking system suppliers, such as Knorr Bremse, have also been developing new brake controllers with deceleration control functions in recent years [26,27].

In this paper, a practical deceleration control algorithm based on the parameter estimation method is proposed and integrated into a bogie-controlled, electro-pneumatic brake controller prototype. We combined all the uncertain parameters into one variable for estimation, which significantly reduces the difficulty of the embedded software programming for the controller. Subsequently, we carried out an engineering-compatible design. Furthermore, to confirm the practicality of the algorithm, the prototype was experimentally verified by a series of ground tests with a test bench.

The research work of this paper is organized as follows. The next section introduces the architecture and the working principle of braking systems. Section 3 gives the deceleration control algorithm. Section 4 presents the compatible design of the software logic. The test bench is introduced, and the test results are presented and discussed in Section 5. Finally, this paper is briefly concluded in Section 6.

2. The Architecture and Working Principle of Braking Systems

At present, the bogie-controlled type is the mainstream braking system used by urban rail vehicles. This system works in a train-level braking force management mode with an electronic brake control unit (EBCU) as the master controller performing the train braking force calculations. The inputs for the braking force calculation are the vehicle load and the braking command, i.e., the target deceleration. Figure 1 shows that the master controller calculates the target braking force and then distributes it to all the controllers mounted near each bogie. Then, each EBCU controls the solenoid valves to generate the pressure so that the pneumatic braking force can be applied.

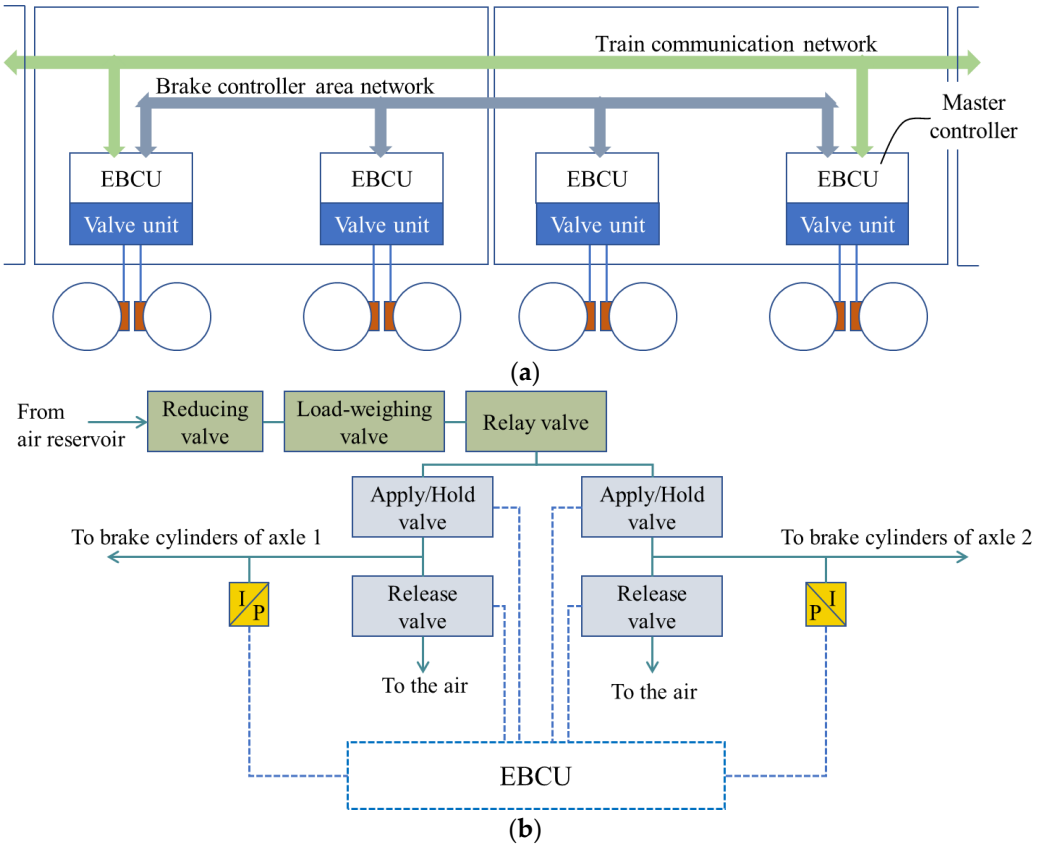

Figure 1. Architecture of the bogie-controlled braking system: (**a**) communication architecture; (**b**) working valves diagram.

Under the conventional braking process control mode (Figure 2a), the target braking force in a non-deceleration control mode is calculated based on the relevant parameters preset in the electronic brake control unit (EBCU). Although this control mode can accurately control the electric braking force and brake cylinder pressure to reach the target value, the actual deceleration may also be affected by uncertain parameters, such as the friction coefficients of brake pads, ramp resistance of the line, and vehicle load. For example, the brake pad friction coefficient often varies with the train speed [28–30]; however, in the EBCU, the brake pad friction coefficient is commonly set as a constant. Thus, in this paper, it is called a non-deceleration control mode.

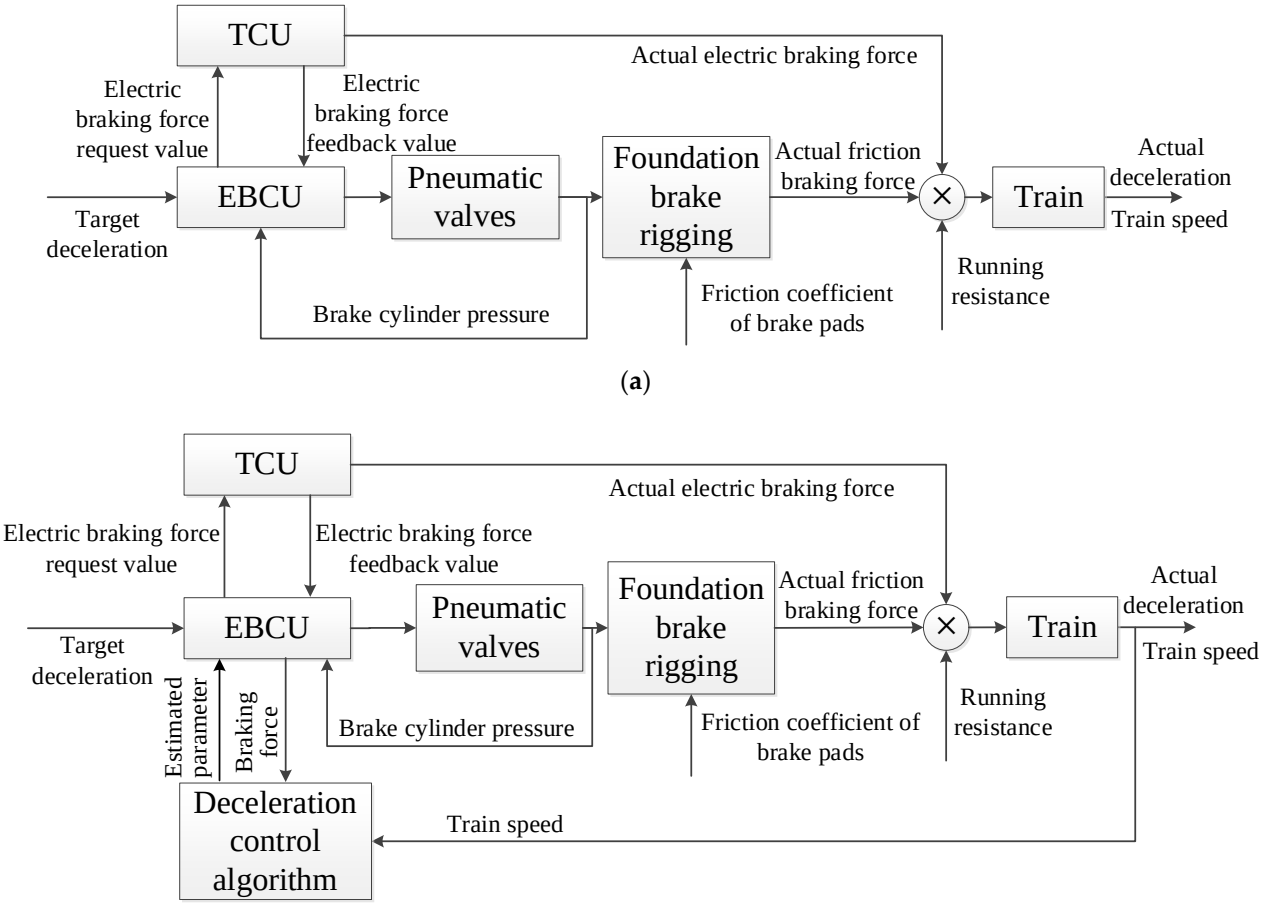

Figure 2. Schematic diagram of the braking control mode: (**a**) conventional non-deceleration control mode; (**b**) deceleration control mode.

To overcome the drawbacks of the non-deceleration control mode, the concept of a deceleration control mode has been developed in the field of brake control. Figure 2b shows the diagram of the deceleration control mode. Unlike the non-deceleration control mode, the deceleration control mode directly takes the actual deceleration or speed as the feedback information and realizes a closed-loop control of the deceleration. In the deceleration control mode, the actual deceleration of the train can be obtained by deriving the train speed or installing an acceleration sensor. Many uncertain parameters in the process of train braking are considered in the closed-loop system so that accurate control of the deceleration can be realized.

3. Deceleration Control Algorithm

For a train, the force that slows it down is the external force. The spring and damping force and the coupler force can be regarded as internal forces, and the train can be regarded as a mass point. At this time, the motion of the train has evolved into the movement of a mass point along the rail. So, a simplified train kinematics model in the braking phase can be described as

$$M\dot{v} + Mg\left(k_1 v^2 + k_2 v + k_3\right) + Mg\sin(\arctan i) + F_{\mathrm{ED}} + F_{\mathrm{EP}} = 0 \quad (1)$$

where v is the train speed; M is the total mass of the train; g is the gravitational acceleration; k_1, k_2 and k_3 denote the coefficients of the basic running resistance; i is the ramp gradient

(positive means uphill); F_{ED} is the total electrodynamic braking force of the train; and F_{EP} is the total electro-pneumatic braking force of the train.

Let $F_B = F_{ED} + F_{EP} = \overline{F}_B + \Delta F$ and $F_R = Mg\left(k_1 v^2 + k_2 v + k_3\right) + Mg\sin(\arctan i)$, and we can obtain

$$M\dot{v} + F_R + \overline{F}_B + \Delta F = 0 \tag{2}$$

$$\overline{F}_B = \sum_{j=1}^{n}\left(p_j A - F_s\right)\delta\eta f_j + \overline{F}_{ED} \tag{3}$$

where F_B is the total braking force; F_R is the total resistance force; $\overline{F}_B$ is the nominal braking force calculated by the control system based on the feedback value of the electric braking force $\overline{F}_{ED}$ and the measured brake cylinder pressure p_j (subscript j means the j-th cylinder); ΔF is the error between the actual value and the nominal value of the braking force due to the uncertain parameters, such as the brake pad friction coefficient, vehicle load or control differences among the cars; A is the effective area of a brake cylinder; F_s is the return spring force; δ is the brake ratio; η is the efficiency; and f_j is the friction coefficient of the j-th brake friction pair.

Equation (2) can be rewritten as

$$\dot{v} + \frac{F_R}{\overline{M}} + \frac{\overline{F}_B}{\overline{M}} + \frac{\Delta F}{\overline{M}} + \xi = 0 \tag{4}$$

where $\overline{M}$ is the nominal vehicle mass obtained by the control system based on the vehicle load transducers; and ξ is the error item containing the error between the nominal value and the real value of the vehicle mass, as well as other unmodeled dynamics.

Redefining $\beta = \frac{F_R}{\overline{M}} + \frac{\Delta F}{\overline{M}} + \xi$, we can obtain

$$\beta = -\frac{\mathrm{d}v}{\mathrm{d}t} - \frac{\overline{F}_B}{\overline{M}} \tag{5}$$

The Laplace transformation of Equation (5) is

$$\beta = -sV(s) - \frac{\overline{F}_B}{\overline{M}} + v(0) \tag{6}$$

where s is the Laplace operator.

To avoid the effect of measurement noise, a first-order filter $\frac{\lambda}{s+\lambda}$ is introduced to the right side of Equation (6). Then, we can obtain

$$\beta = \frac{\lambda}{s+\lambda}\left[-sV(s) - \frac{\overline{F}_B}{\overline{M}} + v(0)\right] \tag{7}$$

$$\beta = -V(s)\lambda + \frac{V(s)\lambda^2 - \lambda\frac{\overline{F}_B}{\overline{M}} + \lambda v(0)}{s+\lambda} = -V(s)\lambda + \phi \tag{8}$$

where $\phi = \frac{V(s)\lambda^2 - \lambda\frac{\overline{F}_B}{\overline{M}} + \lambda v(0)}{s+\lambda}$.

Then, from the inverse Laplace transformation of Equation (8), we can obtain

$$\dot{\phi} + \lambda\phi = \lambda^2 v - \frac{\lambda}{\overline{M}}\overline{F}_B \tag{9}$$

where the initial value is $\phi(0) = \lambda v(0)$.

In Equation (9), v, $\overline{M}$ and $\overline{F}_B$ are measurable inputs; and λ is the cutoff frequency of the first-order filter. Hence, we can obtain ϕ by solving Equation (9). Then, we can obtain the estimated value of β as

$$\hat{\beta} = -\lambda v + \phi \tag{10}$$

Figure 3 shows that, after obtaining the estimated parameter $\hat{\beta}$, the target braking force of the train can be calculated based on the target deceleration a_{target}

$$F_{\text{target}} = \overline{M}\left(a_{\text{target}} - \hat{\beta}\right) \tag{11}$$

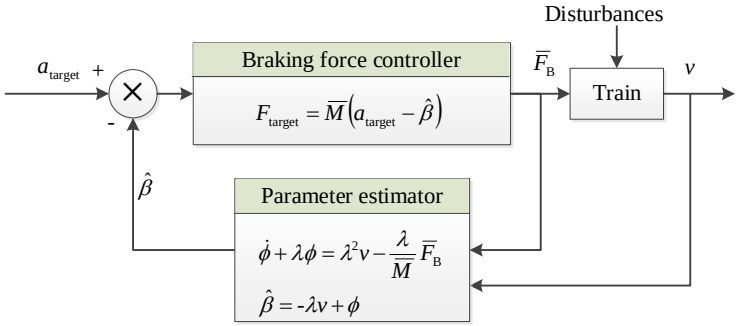

Figure 3. Schematic diagram of the deceleration controller.

Because the deceleration control algorithm should be deployed in the EBCU, the differential Equation (9) should be solved with discrete numerical algorithms, such as the Runge–Kutta method [31].

4. Software Logic Design

To realize the engineering application of the algorithm and to meet the requirements of the braking system, it is necessary to design the specific software logic of the deceleration control.

4.1. Target Braking Force Calculation

In the deceleration control mode, the target braking force can be calculated according to Equation (11). However, there are specific values of $\hat{\beta}$ under certain conditions:

(1) When there is no braking command, $\hat{\beta} = 0$;

(2) Under the conditions of emergency braking and emergency traction, $\hat{\beta} = 0$ because those braking modes are triggered by the hardwires, and there is usually no software computing to guarantee a high safety integrity level.

4.2. Compatible Design of Deceleration Control with Anti-Skid Control

To some extent, the anti-skid control and deceleration control are contradictory. Once one or several axles slide in the deceleration control mode, the braking deceleration of the train may be lower than the target value. At this time, if there is no compatible design of the anti-skid control, the deceleration control algorithm may continue to increase the target braking force, thus aggravating vehicle sliding.

Therefore, as shown in Figure 4, the EBCU needs to collect the sliding states of the entire train (including the sliding during the electric braking and the pneumatic braking) to determine the sliding degree of each axle and implement the following adjustment: When there are one or more axles of the whole train sliding, the estimated value $\hat{\beta}$ can only be increased or maintained, not reduced. In other words, we need to set an output saturation.

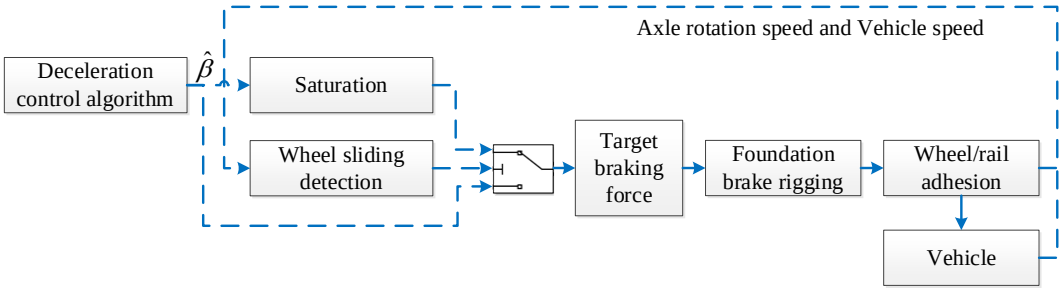

Figure 4. Schematic diagram of the compatible design.

4.3. Setting of the Delay Time

Since the deceleration control algorithm is based on the train braking force and speed, the applied braking force is not yet stable when the braking force starts to increase. Therefore, the deceleration control should be applied after a certain delay time. The delay time in this paper is set to 4 s.

4.4. Optimization of the Dead Zone

To reduce the action times of the electro-pneumatic valves and the regulation frequency of the electric braking force, a control dead zone was set in the deceleration control mode. A common dead zone is when the difference between the actual and target deceleration is less than a certain threshold, and the target braking force remains unchanged at the value of the previous moment. However, this may result in "stages" of the deceleration curve when the target deceleration itself changes. So, in this paper, we designed the dead zone according to the change in the estimated parameter. If the difference between the estimated value $\hat{\beta}$ and the value $\hat{\beta}_{\text{last}}$ of the previous computing cycle is less than c_0, the target braking force does not change, which means the value $\hat{\beta}_{\text{final}}$ in Equation (12) is finally used in the braking force calculation. Based on this optimization, the target deceleration and the estimated parameter can be separated, thereby avoiding the "stages" phenomenon. c_0 in this paper is set to 0.05.

$$\hat{\beta}_{\text{final}} = \begin{cases} \hat{\beta}, & \left|\hat{\beta} - \hat{\beta}_{\text{final\_last}}\right| > c_0 \\ \hat{\beta}_{\text{final\_last}}, & \left|\hat{\beta} - \hat{\beta}_{\text{final\_last}}\right| \le c_0 \end{cases} \tag{12}$$

4.5. Control Flow

Figure 5 shows a flowchart of the deceleration control method. The control logic is designed to match with the existing functions. In this chart, $\hat{\beta}_{\text{last}}$ is the calculated value of $\hat{\beta}$ in the last cycle, and $\hat{\beta}_{\text{final\_last}}$ is the calculated value of $\hat{\beta}_{\text{final}}$ in the last cycle.

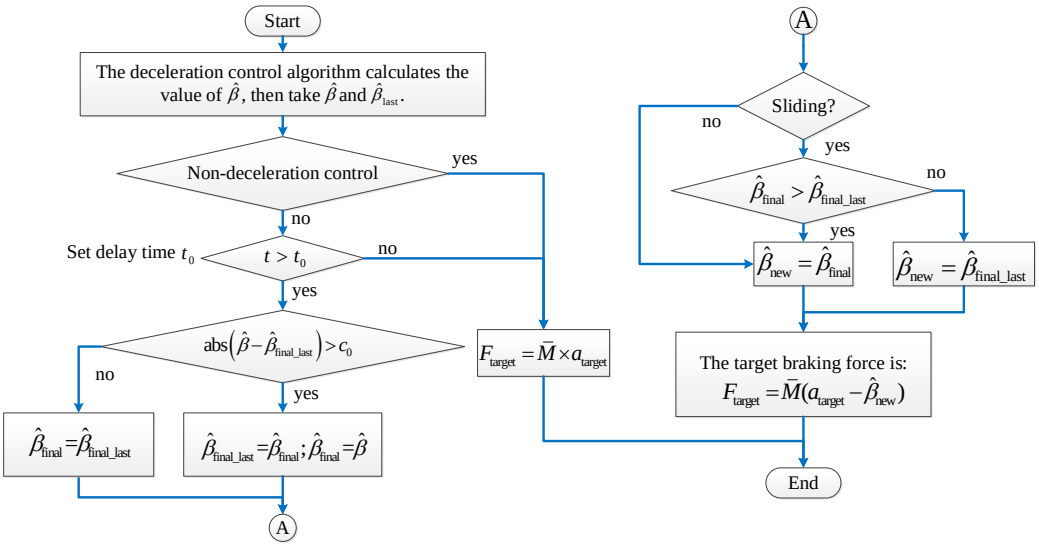

Figure 5. Deceleration control flow chart.

5. Test Verification with a Ground Combined Test Bench

To verify the robustness and reliability of the designed deceleration control function for the brake controller prototype, a hardware-in-the-loop (HIL) experiment platform is established.

5.1. Test Bench

5.1.1. Hardware

The test bench used in this paper is a ground-combined test bench of the braking system, which has a large hardware apparatus in the loop (Figure 6). The test bench can provide the test environment for braking systems of sizes up to an eight-car marshaling train. The pneumatic circuits of the test bench are equivalent to the actual vehicle with the braking devices and equal-volume air cylinders equipped to simulate the actual conditions of the train. The test bench's console includes a network computer, remote monitoring computer and control computer. The computers are connected through the local area network to enable a seamless exchange of data between the components. Among them, the network computer and control computer are used to implement the hardwires and the multifunction vehicle bus (MVB) network connections between the console and the EBCUs. The control computer is used for sending command signals and processing real-time running data, thus providing a virtual train with a simulated operation environment for the braking test. Additionally, the monitoring computer acquires all the transducers and uploads the values to the local area network.

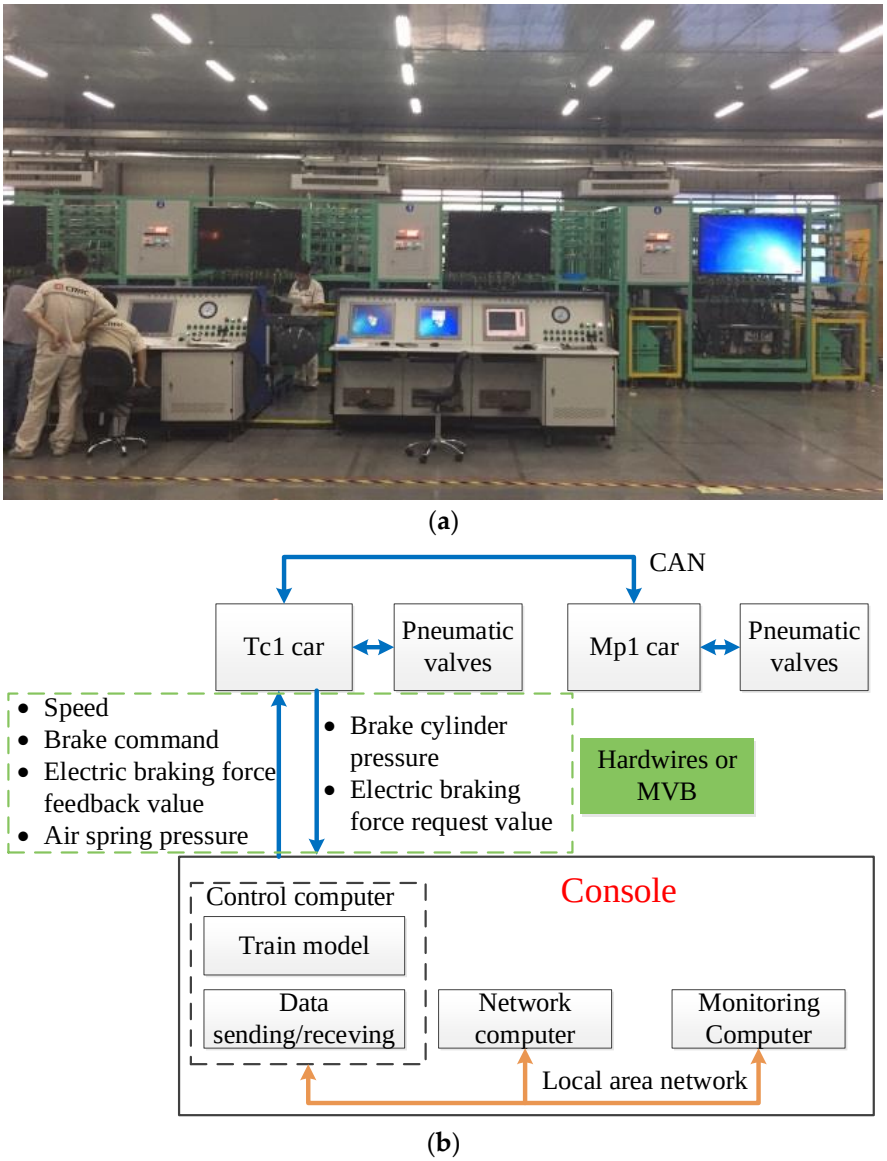

Figure 6. Ground-combined test bench: (**a**) photograph; (**b**) schematic diagram.

In this paper, a dynamic train model that includes one motor car and one trailer is adopted. The braking system, named EPBD-50, is bogie-controlled. It is a new product from the CRRC Nanjing Puzhen Haitai brake equipment corporation. The photograph of the brake controller prototype integrated with the deceleration control function is shown in Figure 7. This deceleration control software is integrated into the braking force management card of the EBCU. Each motor car and trailer are equipped with two EPBD-50 devices, and they communicate with each other through the controller area network (CAN). To match the deceleration control and existing functions, such as the network communication, anti-skid control and other functions, only the target braking force calculation code is modified in the prototype with the hardware remaining unchanged.

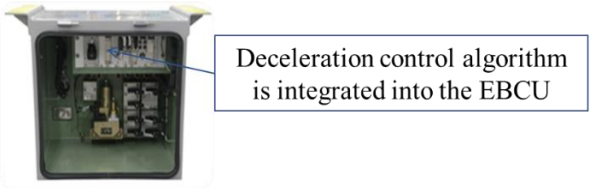

Figure 7. Brake controller prototype integrated with deceleration control function.

5.1.2. Software

The host software is deployed in the control computer and the network computer of the ground-combined test bench. Figure 8 shows the signal transmission between the software and the hardware. The software, including the graphical user interface, train dynamics model and traction control unit (TCU) model, is developed with LabVIEW. The train dynamics model provides the EBCU with the vehicle load and axle speed information. MVB and hardwires are used to communicate with the EBCU in the brake controller prototype. The EBCU calculates the target braking force according to the received signals and decides the target braking pressure, subsequently sending out control signals to the pneumatic valve units to charge and discharge the brake cylinders.

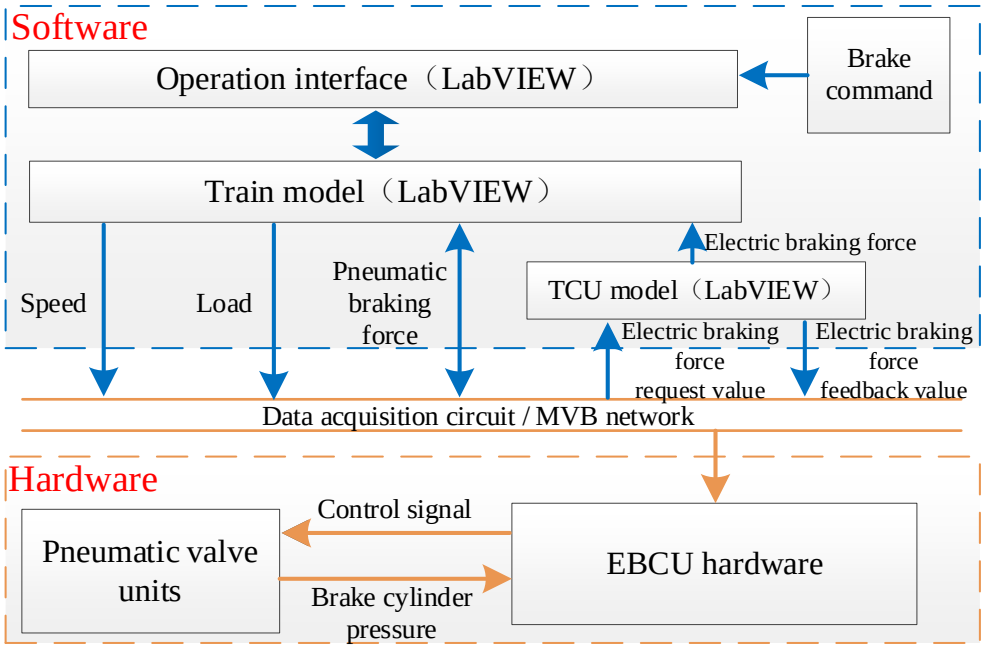

Figure 8. Software and hardware communication topology.

5.2. Test Results and Discussion

Based on the ground-combined test bench, the functions of the brake controller prototype with deceleration control were validated. The controlling performance of the deceleration control algorithm was verified by varying the uncertain parameters, such as the brake pad friction coefficient, ramp gradient, vehicle load and braking force feedback errors. The functional integrity of the deceleration control prototype was further verified by conducting an anti-skid test and an automatic train operation (ATO) mode parking test.

5.2.1. Test without Uncertain Parameters

The test without uncertain parameters means that the parameters set for the train model are the same as the preset parameters in the EBCU. The objective is to explore whether the deceleration control would have a negative impact on the existing system and to check the test environment.

The vehicle model parameters used in the test were from a train serving on an inter-city metro line in China. Table 1 lists the theoretical deceleration of the train, which gives the definition of the target braking deceleration under different braking levels. The vehicle weight was set to the AW3 (overloaded) condition, and the initial test speed was set to 140 km/h. The brake pad friction coefficient was set to 0.36 for the trailer and 0.34 for the motor car.

Table 1. Theoretical deceleration definition in the test.

Theoretical Deceleration (m/s^2)	**Running Speed of the Train (v)**			
	0–5 km/h	**5–20 km/h**	**20–80 km/h**	**80–140 km/h**
Full-service braking	-0.9391	$-0.015727 \times v - 0.8605$	-1.175	$0.004333 \times v - 1.5217$
Fast braking		-1.28		
Emergency braking		-1.28		

As the deceleration control function does not work under emergency braking condition, Figure 9 shows the test results of pure pneumatic full-service braking and electro-pneumatic fast braking. There is no evident difference between the non-deceleration and deceleration control modes without any uncertain parameters (Table 2). The difference in the average deceleration between the deceleration and non-deceleration controls is less than 0.01 m/s^2. Additionally, the maximum difference between the instantaneous and theoretical decelerations under the two modes is very close with both less than 0.05 m/s^2.

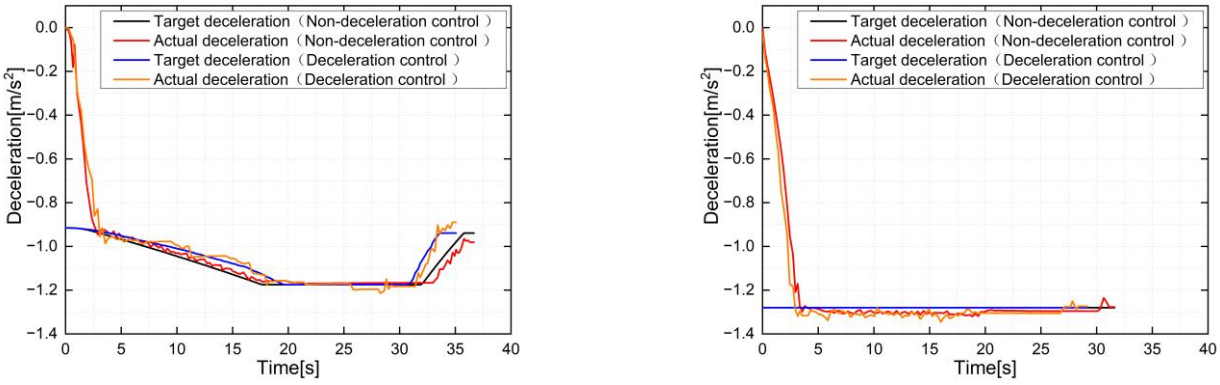

Figure 9. Test results without uncertain parameters: (**a**) pure pneumatic full-service braking; (**b**) electro-pneumatic fast braking.

Table 2. Test results of Figure 9.

	Average Deceleration		Maximum Difference of Instantaneous Deceleration [1]	
	Deceleration Control	**Non-Deceleration Control**	**Deceleration Control**	**Non-Deceleration Control**
Figure 9a	−0.990911	−0.982719	−0.02601	0.042848
Figrue 9b	−1.133771	−1.132026	−0.01701	−0.01838

[1] The calculation range of the difference of instantaneous deceleration is from 8 s after braking initiation to stop.

That means the deceleration control does not negatively affect the calculation of the target braking force or the electric and pneumatic braking force distributions when there are no uncertain parameter disturbances. Therefore, the deceleration control will not affect the original braking performance of the braking system.

5.2.2. Test with Uncertain Parameters

In the test with uncertain parameters, except for the interference parameters, the other parameters were consistent with the test in Section 5.2.1. The uncertain parameters include the brake pad friction coefficient, ramp gradient, vehicle load, braking force feedback error and a combination of them.

(1) Influence of the brake pad friction coefficient

In the braking force calculation process, the brake pad friction coefficient is a conversion coefficient between the braking force and the brake cylinder pressure. The current non-deceleration control is only for the closed loop of the brake cylinder pressure to ensure that the brake cylinder pressure is consistent with the target pressure. However, the actual conversion from the brake cylinder pressure to the applied braking force cannot be directly monitored. Therefore, if the brake pad friction coefficient is affected by running speed, surface contamination and/or other factors, its actual value is not equal to the pre-set value in the EBCU. In this case, the actual braking force will become lower or higher.

Figure 10 shows the test results of the uncertain brake pad friction coefficient. Figure 10a is the test result for when the actual brake pad friction coefficient was set to 0.5, and the theoretical value in the EBCU was set to 0.36 for the trailer and 0.34 for the motor car. The test was under a pure pneumatic full-service braking condition. As the non-deceleration control only controls the inner loop of the brake cylinder pressure, the actual deceleration was higher than the target value during the entire process because of a higher friction coefficient. Table 3 shows that the maximum difference in the instantaneous deceleration under the non-deceleration control mode is approximately 0.5 m/s^2. Additionally, the actual deceleration requires some time to be built up after braking begins; hence, the deceleration control algorithm was not used in the first 4 s (during which the braking force was applied based on the non-deceleration control mode). After 4 s of braking, the braking force was applied, and the $\hat{\beta}$ value of the deceleration control algorithm converged to a stable value. At that time, the deceleration control was used to adjust the braking force, and the actual deceleration could accurately track the target braking deceleration. Table 3 shows that the maximum difference in the instantaneous deceleration under the deceleration control mode is less than 0.05 m/s^2.

The braking condition of Figure 10b is also a pure pneumatic full-service braking. The brake pad friction coefficient was set to vary with the train speed as $f = 0.43 - 0.0003 \times v$. It was found that the deceleration control could likewise make the actual braking deceleration accurately track the target value and perform continuous adjustments. However, the actual braking force during the entire process was also too high, so the non-deceleration control lost the deceleration accuracy.

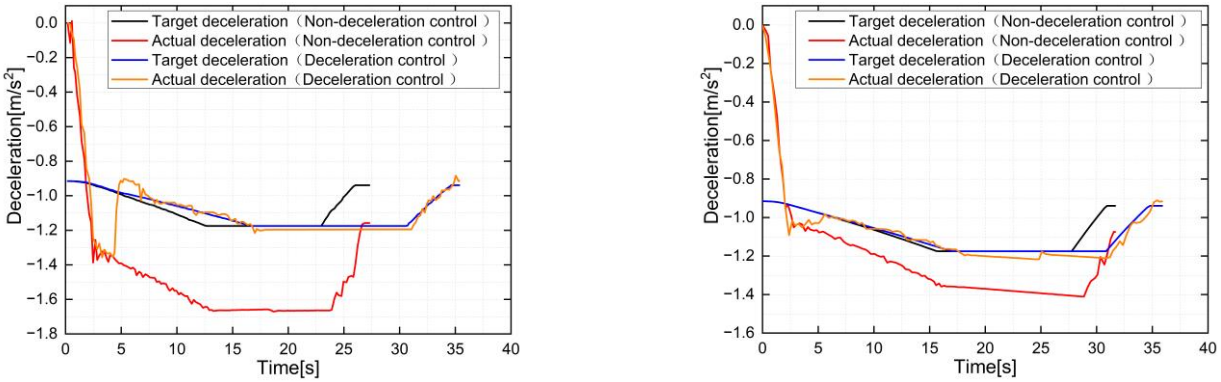

Figure 10. Test results with uncertain brake pad friction coefficient: (**a**) the brake pad friction coefficient is 0.5; (**b**) the brake pad friction coefficient is $f = 0.43 - 0.0003 \times v$ (v is the train speed).

Table 3. Test results of each condition.

Results	Difference of Average Deceleration		Maximum Difference of Instantaneous Deceleration [1]	
	Deceleration Control	Non-Deceleration Control	Deceleration Control	Non-Deceleration Control
Figure 10a	−0.02343	0.29539	0.034695	0.498566
Figure 10b	−0.04713	0.05048	0.042405	0.229123
Figure 11a	0.03656	0.20393	−0.02743	0.228948
Figure 11b	−0.07623	0.03648	0.117281	0.264435
Figure 12	−0.0248	0.18829	0.119957	0.35455
Figure 13a	−0.09472	−0.13709	0.080415	0.114267
Figure 13b	−0.03343	−0.06117	−0.02323	−0.08865
Figure 14	−0.06408	0.13107	0.113254	0.385273

[1] The calculation range of the difference of instantaneous deceleration is from 8 s after braking initiation to stop.

(2) Influence of the line ramp

The ramp of the line is an inconstant external interference, so the non-deceleration control mode cannot deal with the influence of the ramp gradient. However, the deceleration control mode can realize the closed-loop control of the actual deceleration through parameter estimation; thus, the influence of the ramp gradient can be reduced.

Figure 11 shows the ramp influence on the test results. The test was under a pure pneumatic full-service braking condition. Figure 11a shows the comparison between the deceleration control and the non-deceleration control on a 25% uphill line. Figure 11b shows the result of a varying gradient ramp in which the gradient is continuously changing. There was no ramp for the first 150 m after the train started to brake. Then, the gradient increased from 0 to 30% for the next 150 m in which the vertical curve radius was 5000 m. Then, the gradient remained constant for the next 200 m. Additionally, the gradient then decreased from 30% to 0 for the next 150 m. Finally, the gradient remained constant at 0. From the comparison, the actual deceleration changes were completely based on the ramp gradient in the non-deceleration control mode, whereas the deceleration control mode could implement certain compensations for the ever-changing gradient value.

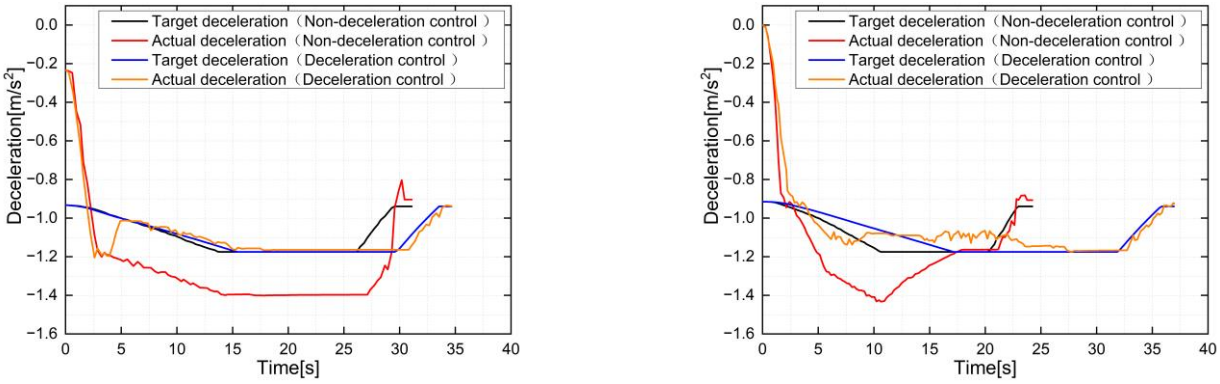

Figure 11. Test results with uncertain ramp gradient: (**a**) 25% gradient uphill ramp; (**b**) varying gradient ramp.

(3) Influence of the vehicle load

The effect of the uncertain vehicle load is similar to the brake pad friction coefficient. The load value is acquired with the EBCU and may be different from the actual value in some failure cases.

The vehicle load in the test was set to an extreme condition to simulate the event of the air spring sensor failure, i.e., the vehicle load in the EBCU software and the train model were set as AW3 and AW0 (empty load), respectively. The test was under a pure pneumatic full-service braking condition. Figure 12 shows that the deceleration control under the test condition could estimate the actual vehicle weight and then apply the matching braking force, while the actual deceleration under the non-deceleration control mode was too high.

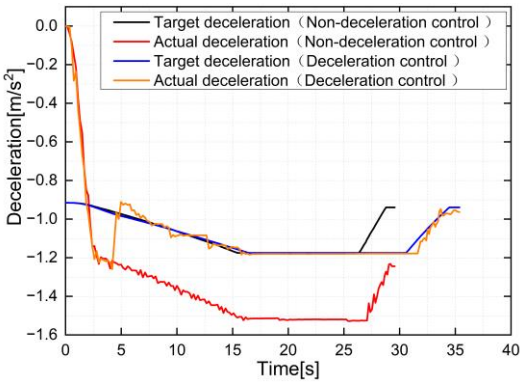

Figure 12. Test result with an uncertain load.

(4) Influence of the braking force feedback error

The braking force feedback error mainly includes the brake cylinder pressure sensor error, i.e., the pneumatic braking force feedback error, and the electric braking force feedback error. If there are errors in the brake cylinder pressure and the feedback value of the electric braking force, the actual deceleration under the non-deceleration control will deviate from the target value (Figure 13), while the deceleration control can compensate for the influence of the error.

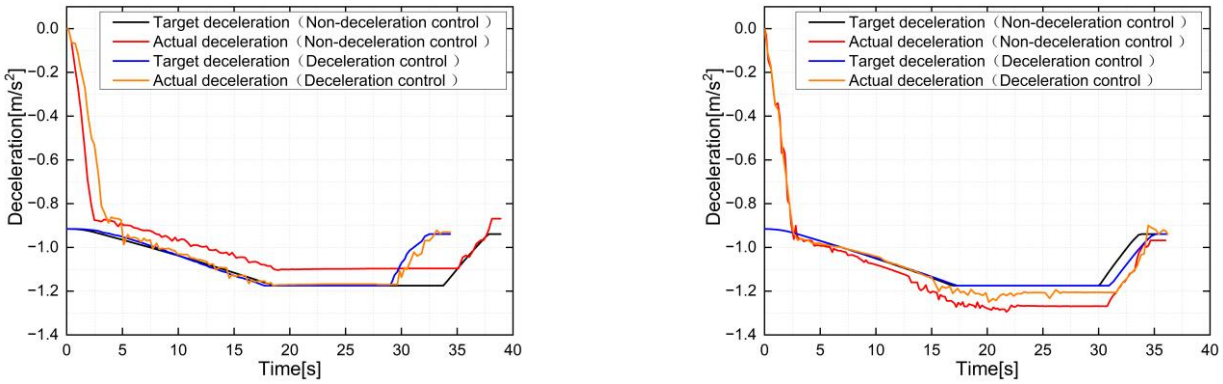

Figure 13. Test results with uncertain braking force feedback errors: (**a**) brake cylinder pressure sensor error is 5% under a pure pneumatic full-service braking condition; (**b**) electric braking force feedback error is 10% under an electro-pneumatic full-service braking condition.

(5) Influence of a combination of uncertain parameters

In the presence of some uncertain parameters in the braking process that affect the train's actual deceleration, all the disturbances are reflected in the estimated value $\hat{\beta}$ with the deceleration control method. Therefore, the errors affecting the actual deceleration of the train can be compensated. Figure 14 shows a comparison between the deceleration control and the non-deceleration control with a combination of uncertain parameters. Even in this case, the actual deceleration of the deceleration control mode could still efficiently follow the target deceleration.

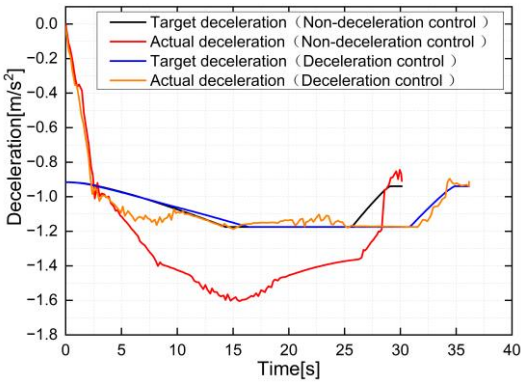

Figure 14. Test result with a combination of uncertain parameters.

Table 3 shows the actual average deceleration and the maximum difference in instantaneous deceleration. The average deceleration in the deceleration control mode was relatively stable, and the instantaneous deceleration control error was smaller. Comparing the two control modes, we conclude that the deceleration control mode is better than the non-deceleration control for both instantaneous and average deceleration.

5.2.3. Anti-Skid Matching Test

Based on the anti-skid-compatible design described in Section 4.2, when one or more axles are sliding in a train, $\hat{\beta}$ can only be increased or maintained but not reduced. An anti-skid matching test was conducted. The braking condition was pure pneumatic full-service braking, and the adhesion coefficient was set as a low-adhesion condition [32]. The available adhesion coefficient was lower than that required by the target deceleration; therefore, the vehicle kept sliding during the whole braking process. Figure 15 shows that there is no evident difference between the deceleration control and the non-deceleration control.

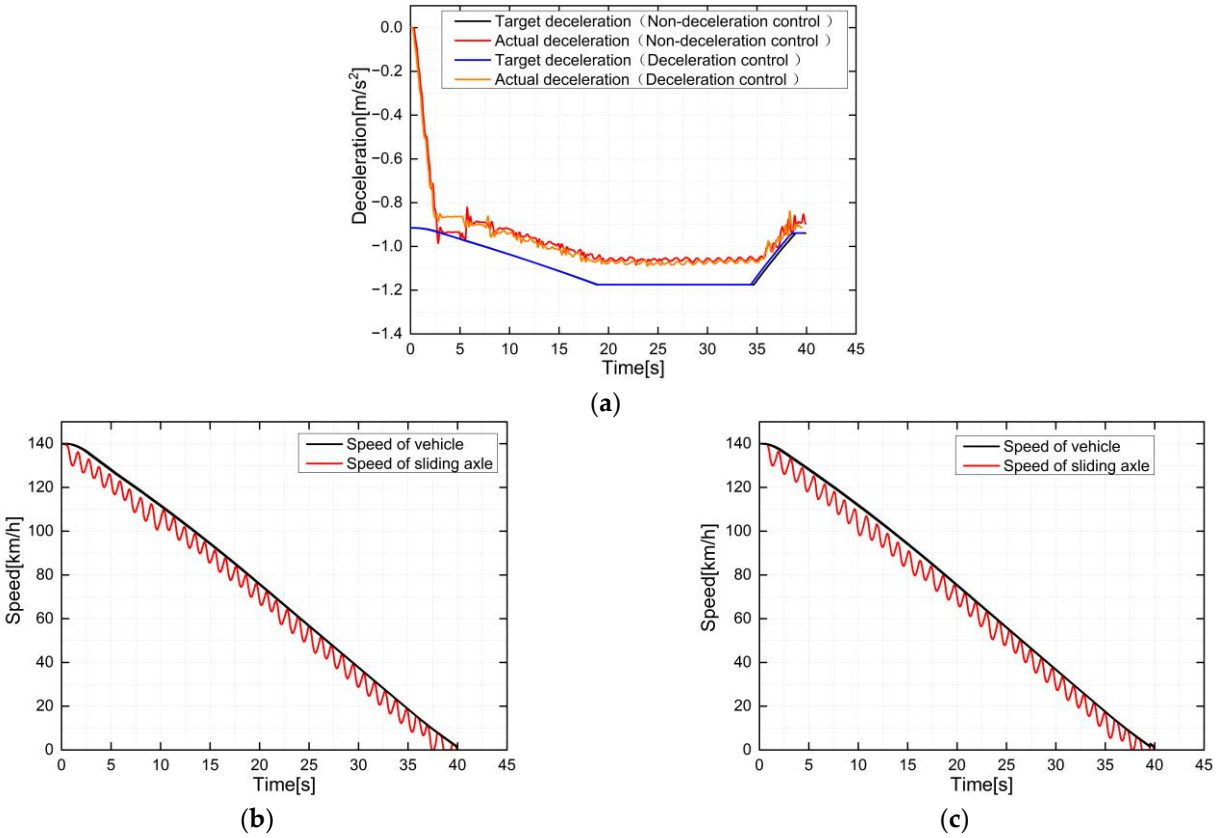

Figure 15. Anti-skid matching test results: (**a**) braking deceleration; (**b**) sliding axle speed under the non-deceleration control mode; (**c**) sliding axle speed under the deceleration control mode.

5.2.4. ATO Mode Parking Test

The ATO mode parking test is conducted to indirectly verify the response performance of the deceleration control algorithm when the metro train stops at stations. On this occasion, the braking command has frequent adjustments. The signal sent by the ATO system in the actual vehicle operation process from a Shanghai metro line was selected, and the braking command data was inquired as the braking command input in this test.

The test results are shown in Figure 16. It can be found that the deceleration control could fully track the ATO braking command and was not inferior to the non-deceleration control in terms of response characteristics. Therefore, the deceleration control algorithm can be used in the ATO mode.

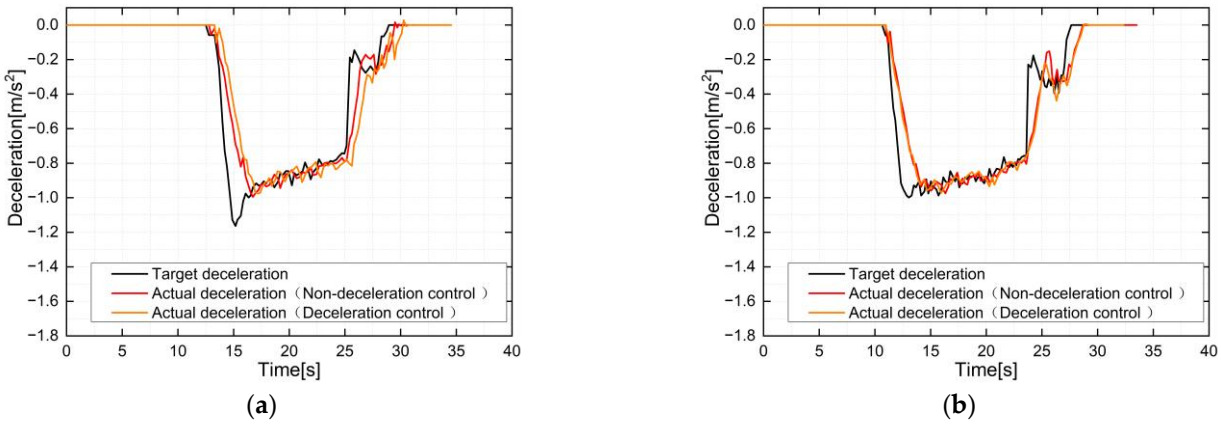

Figure 16. ATO mode parking test results: (**a**) Test 1; (**b**) Test 2.

In addition, the braking force should be accurately adjusted in the deceleration control mode, which requires frequent action of the electro-pneumatic valves. Table 4 lists the action times of the electro-pneumatic valves under the non-deceleration control and the deceleration control modes. Compared with the non-deceleration control mode, the maximum increment rate of the action times under the deceleration control mode was 36%. This increment is within the acceptable range and will not significantly affect the valve lifespan.

Table 4. Action times of the electro-pneumatic valves.

Type of Tests	Counts of Test Groups	Action Times Under Non-Deceleration Control Mode	Action Times under Deceleration Control Mode	Rate of Change
Influence of brake pad friction coefficient	48	2785	3512	26%
Influence of line ramp	84	4700	6061	29%
Influence of vehicle load	24	485	573	18%
Influence of electric braking force feedback error	12	856	1168	36%
Influence of brake cylinder pressure sensor error	24	1301	1662	28%
Influence of a combination of uncertain parameters	12	683	929	36%
Anti-skid matching test	84	11,243	12,371	10%
ATO mode parking test	4	630	650	3%

6. Conclusions

The braking control mode for metro trains is still an open loop in terms of train deceleration, meaning performance is not good enough when there are external disturbing factors. A deceleration control algorithm based on parameter estimation was studied in this work; therefore, it was an application-oriented study to solve a real-world control problem. For the engineering application and the matching issue with the existing braking system functions, some key design details are also discussed in this paper. Finally, the proposed control algorithm was integrated into a brake control prototype and was validated by using a ground-combined test bench. The main conclusions of this paper are as follows.

(1) Based on the working principle of the deceleration control, an algorithm based on the parameter estimation method was derived. All the uncertain parameters can be described in a single parameter termed β. The implementation of the deceleration control relies mainly on parameter estimation and the corresponding adjustment of the target braking force.

(2) For engineering applications, a software logic of the deceleration control compatible with other braking control functions was designed. The estimated parameters under specific conditions, interaction with anti-skid control, delay time and dead zone were all considered in the compatible design.

(3) The deceleration control mode was evidently better than the non-deceleration control mode in the presence of the brake pad friction coefficient, ramp, load, sensor errors or their combined effect. Additionally, the deceleration control function did not affect the original performance of the braking system.

(4) The deceleration control method could reduce the deviation between the actual and target deceleration. The average deceleration in the deceleration control mode was relatively stable, and the instantaneous deceleration control error was smaller. However, the braking force will be frequently regulated. The maximum increment rate of the action times of the electro-pneumatic valves was 36%. Therefore, the impact on the electro-pneumatic valves should be analyzed in the future, and further optimization can be carried out to reduce the working frequency of the valves.

Author Contributions: Conceptualization, M.W. and C.T.; methodology, T.M.; software, T.M.; validation, T.M., J.Z. and Y.L.; formal analysis, T.M.; investigation, T.M.; resources, C.T. and Y.L.; data curation, J.Z.; writing—original draft preparation, T.M. and J.Z.; writing—review and editing, T.M.; visualization, T.M. and J.Z.; supervision, C.T.; project administration, M.W. and Y.L.; funding acquisition, M.W. All authors have read and agreed to the published version of the manuscript.

Funding: This research was funded by the China Postdoctoral Science Foundation, grant number 2021M702476, and the National Natural Science Foundation of China, grant number 52072266 and U1534205.

Data Availability Statement: Not applicable.

Acknowledgments: The study is supported by the CRRC Nanjing Puzhen Haitai Brake Equipment Co., Ltd., Nanjing, China. The authors are grateful for the help.

Conflicts of Interest: The authors declare no conflict of interest.

References

1. Boynukalin, S.; Açikbaş, S.; Söylemez, M.T. Effect of guaranteed emergency braking rate and gradient on turnback headway time in metro lines. In Proceedings of the 2021 13th International Conference on Electrical and Electronics Engineering (ELECO), Bursa, Turkey, 25–27 November 2021; pp. 52–56.
2. Thurston, D.F. Deceleration rates for safe braking distance calculations. In Proceedings of the 2017 Joint Rail Conference. American Society of Mechanical Engineers Digital Collection, Philadelphia, PA, USA, 4–7 April 2017.
3. *IEEE 1698-2009*; IEEE Guide for the Calculation of Braking Distances for Rail Transit Vehicles. IEEE: Piscataway, NJ, USA, 2009.
4. Wu, M.; Cheng, G.; Wang, X. Discussion of braking deceleration control of railway vehicle. *J. China Railw. Soc.* **2009**, *31*, 94–97.
5. Wu, M.; Ma, T.; Yang, J.; Chen, M. Discussion on development trend of train braking technology. *China Railw. Sci.* **2019**, *40*, 134–144.
6. Nankyo, M.; Ishihara, T.; Inooka, H. Feedback control of braking deceleration on railway vehicle. *J. Dyn. Syst. Meas. Control.* **2006**, *128*, 244–250. [CrossRef]
7. Nankyo, M.; Ishisara, T.; Inooka, H. Feedback control of brake system on railway vehicle considering nonlinear property and dead time. In Proceedings of the International Mechanical Engineering Congress and Exposition, Washington, DC, USA, 15–21 November 2003; pp. 99–104.
8. Nankyo, M.; Nakazawa, S.; Nanaka, T.; Yoshikawa, H. Development of a braking system equipped with deceleration feedback control. *RTRI Rep.* **2009**, *23*, 41–46.
9. Nakazawa, S. Accuracy improvement of braking distance by deceleration feedback function applying to brake system. *Q. Rep. RTRI* **2021**, *62*, 167–172. [CrossRef]
10. Wu, M.; Chen, C.; Tian, C.; Zhou, J. Precise train stopping algorithm based on deceleration control. In Proceedings of the 5th International Conference on Intelligent Transportation Engineering (ICITE), Beijing, China, 11–13 September 2020; IEEE: Piscataway, NJ, USA, 2020; pp. 281–284.
11. Wu, M.; Luo, Z. Study on train braking deceleration feedback control based on adaptive parameter estimation. *J. China Railw. Soc.* **2015**, *37*, 8–16.
12. Luo, Z.; Cao, H.; Zhang, Y.; Jiang, Y.; Wen, X.; An, Z.; Li, B. A more accurate two-level robust braking control method on high-speed EMUs. *Railw. Locomot. Car* **2021**, *41*, 169–174.
13. Zhou, J.; Wu, M.; Liu, Y.; Tian, C. Train braking deceleration control based on improved smith estimator. *J. Tongji Univ.* **2020**, *48*, 1657–1667.
14. Ma, T.; Wu, M.; Tian, C. Deceleration-feedback braking force closed-loop control method for urban rail train. *Chin. J. Sci. Instrum.* **2021**, *42*, 197–205.
15. Zhang, M.; Xu, H. Design of urban rail vehicle brake controller based on Krasovskii functionals. *J. Jilin Univ. Eng. Technol. Ed.* **2015**, *45*, 104–111.
16. Yin, J.; Chen, D.; Li, L. Intelligent train operation algorithms for subway by expert system and reinforcement learning. *IEEE Trans. Intell. Transp. Syst.* **2014**, *15*, 2561–2571. [CrossRef]
17. Wang, L.; Wang, X.; Liu, G.; Xu, C. An improved predictive function control algorithm for velocity curve of urban rail vehicle. *Chin. J. Sci. Instrum.* **2022**, *43*, 273–283.
18. Wang, L.; Wang, X.; Sheng, Z.; Lu, S. Model predictive controller based on online obtaining of softness factor and fusion velocity for automatic train operation. *Sensors* **2020**, *20*, 1719. [CrossRef] [PubMed]
19. Tan, C.; Li, Y.; Yang, H. Adaptive braking control for high-speed trains with disturbances and time delays. *J. East China Jiaotong Univ.* **2021**, *38*, 64–71.
20. Li, Z.; Yang, H.; Liu, M.; Liu, J. Modeling and tracking control for braking process of high speed electric multiple unit. *China Railw. Sci.* **2016**, *37*, 80–86.
21. Nie, Y.; Liu, Y.; Cheng, S.; Mei, M.; Xiao, L. Unified brake service by a hierarchical controller for active deceleration control in an electric and automated vehicle. *Energies* **2017**, *10*, 2052. [CrossRef]
22. Luo, Z.; Wu, M.; Zuo, J. Sliding mode pressure controller for an electropneumatic brake: Part II—Parameter identification and controller tests. *Proc. Inst. Mech. Eng. Part I J. Syst. Control. Eng.* **2018**, *232*, 583–591. [CrossRef]
23. Luo, Z.; Wu, M.; Zuo, J. Sliding mode pressure controller for an electropneumatic brake: Part I—Plant model and controller design. *Proc. Inst. Mech. Eng. Part I J. Syst. Control. Eng.* **2018**, *232*, 572–582. [CrossRef]

24. Luo, Z.; Wu, M.; Zuo, J.; Tian, C. Modelling and model validation of an electropneumatic brake on subway trains. *Proc. Inst. Mech. Eng. Part F J. Rail Rapid Transit* **2016**, *230*, 374–391. [CrossRef]
25. Bu, F.; Tan, H. Pneumatic brake control for precision stopping of heavy-duty vehicles. *IEEE Trans. Control. Syst. Technol.* **2007**, *15*, 53–64. [CrossRef]
26. Zhao, J. Braking control technology of new generation metro vehicle based on deceleration control. *Mod. Urban Transit* **2019**, *16*, 39–46.
27. Kreisel, N.; Friesen, U.; Furtwängler, R.; Braeseke, J.; Ciesielski, D. Verzögerungsgeregeltes fahrzeug ermöglicht ein stabileres bremsverhalten in allen geschwindigkeiten. *ZEVrail* **2020**, *144*, 1–13.
28. Sawczuk, W. Analytical model coefficient of friction (COF) of rail disc brake on the basis of multi-phase stationary tests. *Eksploat. I Niezawodn. Maint. Reliab.* **2017**, *20*, 57–67. [CrossRef]
29. UIC 541-3. *Brakes-Disc Brakes and Their Application-General Conditions for the Certification of Brake Pads*; International Union of Railways: Paris, France, 2017.
30. Lee, N.; Kang, C. The effect of a variable disc pad friction coefficient for the mechanical brake system of a railway vehicle. *PLoS ONE* **2015**, *10*, e0135459. [CrossRef]
31. Akinsola, V. *Numerical methods: Euler and Runge-Kutta. Qualitative and Computational Aspects of Dynamical Systems*; IntechOpen: London, UK, 2023.
32. Polach, O. Creep forces in simulations of traction vehicles running on adhesion limit. *Wear* **2005**, *258*, 992–1000. [CrossRef]